Sini Heinonen,[1] Jana Buzkova,[2] Maheswary Muniandy,[1] Risto Kaksonen,[1,3] Miina Ollikainen,[4] Khadeeja Ismail,[4] Antti Hakkarainen,[5] Jesse Lundbom,[5,6] Nina Lundbom,[5] Katriina Vuolteenaho,[7] Eeva Moilanen,[7] Jaakko Kaprio,[8,9,10] Aila Rissanen,[1,11] Anu Suomalainen,[2,12] and Kirsi H. Pietiläinen[1,8,13]

Impaired Mitochondrial Biogenesis in Adipose Tissue in Acquired Obesity

Diabetes 2015;64:3135–3145 | DOI: 10.2337/db14-1937

Low mitochondrial number and activity have been suggested as underlying factors in obesity, type 2 diabetes, and metabolic syndrome. However, the stage at which mitochondrial dysfunction manifests in adipose tissue after the onset of obesity remains unknown. Here we examined subcutaneous adipose tissue (SAT) samples from healthy monozygotic twin pairs, 22.8–36.2 years of age, who were discordant (ΔBMI >3 kg/m^2, mean length of discordance 6.3 ± 0.3 years, *n* = 26) and concordant (ΔBMI <3 kg/m^2, *n* = 14) for body weight, and assessed their detailed mitochondrial metabolic characteristics: mitochondrial-related transcriptomes with dysregulated pathways, mitochondrial DNA (mtDNA) amount, mtDNA-encoded transcripts, and mitochondrial oxidative phosphorylation (OXPHOS) protein levels. We report global expressional downregulation of mitochondrial oxidative pathways with concomitant downregulation of mtDNA amount, mtDNA-dependent translation system, and protein levels of the OXPHOS machinery in the obese compared with the lean co-twins. Pathway analysis indicated downshifting of fatty acid oxidation, ketone body production and breakdown, and the tricarboxylic acid cycle, which inversely correlated with adiposity, insulin resistance, and inflammatory cytokines. Our results suggest that mitochondrial biogenesis, oxidative metabolic pathways, and OXPHOS proteins in SAT are downregulated in acquired obesity, and are associated with metabolic disturbances already at the preclinical stage.

Adipocytes are important contributors to energy balance and metabolic homeostasis. Within these highly dynamic cells, mitochondria are at the center of energy metabolism, using carbohydrates, lipids, and proteins to produce ATP and metabolites for growth, as well as contributing to adipocyte differentiation and maturation (1). Mitochondria possess their own multicopy genome, a 16.6-kb circular mitochondrial DNA (mtDNA) that encodes two ribosomal RNAs (12S and 16S), 22 transfer RNAs, and 13 polypeptides (2). These proteins are the core catalytic components of electron transport chain complexes I, III, and IV, and ATP synthase (3). Together, these complexes form the oxidative phosphorylation (OXPHOS) system in the inner mitochondrial membrane. mtDNA-encoded proteins are translated on mitochondrial ribosomes that, together with OXPHOS complexes, are the only cellular entities encoded by both nuclear and mitochondrial genomes. However, ~1,500 other nuclear-encoded proteins—8% of all nuclear genes—encode mitochondrial

[1]Obesity Research Unit, Research Programs Unit, Diabetes and Obesity, University of Helsinki, Helsinki, Finland
[2]Research Programs Unit, Molecular Neurology, Biomedicum-Helsinki, University of Helsinki, Helsinki, Finland
[3]Siluetti Hospital, Helsinki, Finland
[4]Department of Public Health, University of Helsinki, Helsinki, Finland
[5]Helsinki Medical Imaging Center, University of Helsinki, Helsinki, Finland
[6]Institute for Clinical Diabetology, German Diabetes Center, Leibniz Center for Diabetes Research, Heinrich Heine University, Düsseldorf, Germany
[7]The Immunopharmacology Research Group, University of Tampere School of Medicine and Tampere University Hospital, Tampere, Finland
[8]Institute for Molecular Medicine Finland, University of Helsinki, Helsinki, Finland
[9]Finnish Twin Cohort Study, Department of Public Health, Hjelt Institute, University of Helsinki, Helsinki, Finland
[10]National Institute for Health and Welfare, Department of Mental Health and Substance Abuse Services, Helsinki, Finland
[11]Department of Psychiatry, Helsinki University Central Hospital, Helsinki, Finland
[12]Department of Neurology, Helsinki University Central Hospital, Helsinki, Finland
[13]Abdominal Center, Endocrinology, Helsinki University Central Hospital and University of Helsinki, Helsinki, Finland

Corresponding author: Kirsi H. Pietiläinen, kirsi.pietilainen@helsinki.fi.

Received 23 December 2014 and accepted 8 May 2015.

This article contains Supplementary Data online at http://diabetes.diabetesjournals.org/lookup/suppl/doi:10.2337/db14-1937/-/DC1.

S.H. and J.B. share first authorship.

targeted proteins, emphasizing the central role of mitochondria in cellular metabolism (4).

Evidence from various study systems suggests that mitochondrial function and biogenesis are compromised in subcutaneous adipose tissue (SAT) in type 2 diabetes (5), morbid obesity (6), and insulin resistance (7). Recently, a reduction of total oxygen consumption rates, but not mtDNA content, was shown to occur in visceral and subcutaneous adipocytes of obese adults (8), as well as after β-adrenergic stimulation (9), suggesting a decrease in mitochondrial oxidative activity. We have previously shown in SAT of monozygotic (MZ) weight-discordant twin pairs that mtDNA depletion together with the downregulation of mitochondrial branched-chain amino acid (BCAA) catabolism characterize obesity, insulin resistance, fatty liver (10), and poor fitness (11). However, we still lack a thorough understanding of how mitochondrial biogenesis and function in human adipose tissue changes in obesity, at which stage this process begins, and whether it contributes to the early development of metabolic disturbances. Moreover, it is not known whether the possible link between mitochondrial dysfunction and obesity-related metabolic disorders is genetic or acquired.

MZ twins discordant for obesity are, despite their different phenotype, completely matched for genetic variants, age, and sex. This allows the research of acquired obesity without interference of genetic and familial factors that confound studies comparing groups of unrelated lean and obese individuals. Here, we focus on rare weight-discordant, healthy, young adult MZ twins to investigate in detail the mitochondrial pathways in SAT and their association with whole-body metabolism in acquired obesity.

RESEARCH DESIGN AND METHODS

Subjects

The current study included 26 rare, healthy MZ pairs discordant for obesity (within-pair difference, ΔBMI ≥3 kg/m^2, n = 9 males, n = 17 females, mean age 29.9 ± 0.6 years), identified from two population-based twin cohorts, FinnTwin16 (n = 2,839 pairs) and FinnTwin12 (n = 2,578 pairs) (12). In addition, 14 MZ twin pairs concordant for BMI (ΔBMI <3 kg/m^2, n = 9 males, n = 5 females, mean age 31.6 ± 0.6 years) were included as control pairs and to provide a wider range of BMI values for transcriptomics analyses. A detailed description of the twin material has been published previously (13,14). Written informed consent was obtained from all participants. The study was approved by the Ethical Committee of the Helsinki University Central Hospital.

Clinical Assessments

Weight and height were measured for the calculation of BMI. Body composition was determined by dual-energy X-ray absorptiometry (Lunar Prodigy software version 8.8; GE Healthcare, Madison, WI) (15), the amount of SAT and visceral adipose tissue (VAT) by MRI, and liver fat by proton magnetic resonance spectroscopy with a 1.5 Tesla MRI imager (Avanto; Siemens, Erlangen, Germany) (13). Physical activity was assessed by the Baecke questionnaire and its three subcompartments (sport, leisure time, and work indexes). Parental weight, height, and age were asked at the twin age of 16 years.

Analytical Measurements

The concentrations of fasting plasma glucose, leptin, adiponectin, and adipsin, and serum hs-CRP were measured, and HOMA insulin resistance and Matsuda insulin sensitivity indexes were calculated, as previously described (16).

SAT Specimens and Analyses

Surgical biopsy samples of abdominal SAT under the umbilicus were obtained under local anesthesia and were snap-frozen in liquid nitrogen. Based on the availability of sample material, the frozen SAT specimens were used for transcriptomics analyses (all 26 discordant and 14 concordant twin pairs), determination of the amount of mtDNA, mtDNA-encoded transcript levels (15 discordant twin pairs), and an OXPHOS protein analysis (seven discordant twin pairs). Twenty-four discordant and 11 concordant twin pairs were available for DNA methylation analyses. Clinical characteristics of the selected and unselected twin pairs were similar. Part of the fresh SAT sample was digested with collagenase, and was used for the measurement and calculation of adipocyte volume and number in all 26 discordant and 14 concordant twin pairs (16). The discordant twin pairs were divided into two groups with regard to hyperplastic and hypertrophic obesity (16).

Transcriptomics and Pathway Analyses

Total RNA was extracted from SAT by the RNeasy Lipid Tissue Mini Kit (Qiagen) and treated with DNase I (Qiagen). Transcriptomics analyses were performed using the Affymetrix U133 Plus 2.0 array and were validated as in the study by Naukkarinen et al. (14). Preprocessing of the expression data was performed using BioConductor and the GC-RMA algorithm. We first analyzed the differentially expressed transcripts genome wide between the obese and the lean co-twins in the discordant pairs by paired moderated t tests (17), and then determined whether they were found in MitoCarta (4), an online atlas of 1,013 human proteins with mitochondrial localization. Forty-nine of the 1,013 MitoCarta protein transcripts were not detectable by the Affymetrix probes, including the 13 mtDNA-encoded OXPHOS transcripts. Identified mitochondrial-related transcripts were further subjected to ingenuity pathway analysis (IPA; Qiagen, Redwood City, CA [www.qiagen.com/ingenuity]) to reveal the pathways and the upstream regulators of the transcripts. Top 10 significant pathways were selected for further examination and for the calculation of overall pathway activity (the mean centroid; Table 3) (10). In addition, the mean centroids were calculated for the expression of the mitochondrial ribosomal protein (MRP) small subunit (MRPS; n = 30 subunits) and the mitochondrial ribosomal protein large subunit (MRPL; n = 50 subunits) (Supplementary Table 4).

DNA methylation values of all probes mapping to the differentially expressed MitoCarta genes and peroxisome proliferator–activated receptor γ coactivator (PGC)-1α were picked from the Illumina HumanMethylation BeadChip. Differential methylation analysis of the cytosine guanine dinucleotide (CpG) sites on these genes was performed by using paired moderated *t* tests (18) in the discordant pairs, and relationships between methylation in significant CpG sites and the expression of their associated genes by Spearman correlations in the individual twins.

DNA Extraction and Analysis of mtDNA Amount

The amount of mtDNA, extracted by the standard phenol/chloroform and ethanol precipitation method, was determined by quantitative real-time PCR (qPCR) of the mitochondrial cytochrome B (*CYTB*) gene normalized to the nuclear amyloid β precursor protein (*APP*) gene (10). The qPCR was performed with 25 ng of total DNA using SYBR Green PCR Master Mix (iQ Custom SYBR Green Supermix; Bio-Rad) according to the manufacturer's instructions. The qPCR data were analyzed by the comparative "ΔΔCt method" (with Bio-Rad CFX Manager version 1.6 software). The primer sequences are available in Supplementary Table 7.

Reverse Transcription and the Measurement of mtDNA-Encoded Transcripts and the Upstream Regulator PGC-1α by quantitative RT-PCR

Total extracted RNA (250 ng) was used to generate cDNA with the Maxima First Strand cDNA Synthesis Kit for quantitative RT-PCR (qRT-PCR) (Thermo Scientific) according to the manufacturer's instructions. Expression levels of mtDNA-encoded 12S rRNA (*MT-RNR1*), 16S rRNA (*MT-RNR2*), and mRNAs (*MT-COX1*, *MT-ND5*, and *MT-CYTB*), normalized with nuclear *18S rRNA*, were analyzed in 1:100 cDNA dilutions by qRT-PCR with the iQ Real-Time PCR Detection System (Bio-Rad) and the comparative ΔΔCt method.

The expression of the upstream regulator *PGC-1α* was validated in a 1:30 dilution with *18S rRNA* as a housekeeping gene. The PGC-1α probes were targeted to 3′ untranslated region of the longest mRNA isoform (ENSG00000109819) that is not shared with other protein coding PGC-1α isoforms. The primer sequences are available in Supplementary Table 7.

Quantitative Western Blot Analysis for OXPHOS Protein Levels

SAT lysates were obtained by homogenization in ice-cold 1% n-dodecyl β-D-maltoside in PBS with protease inhibitors (Roche). Quantitative Western blot analysis was performed with 20 μg of total SAT lysates for measurement of the levels of the following OXPHOS proteins: complex I NDUFA9 (MS111), complex II 70-kDa subunit (MS204), complex III core 2 subunit (MS304), complex IV subunit I (MS404), and complex V subunit α (MS507), as well as porin (Abcam), β-tubulin (Cell Signaling Technology), and actin (Santa Cruz Biotechnology). Antibodies were diluted in 1% BSA/Tris-buffered saline and 0.1% Tween 20 (TBST) at 1:2,000 (CI), 1:5,000 (CII), 1:2,500 (CIII), 1:500 (CIV), and 1:1,000 (porin, tubulin), and incubated at 4°C overnight. Secondary HRP-conjugated anti-mouse or anti-rabbit antibodies (1:10,000; Molecular Probes) were incubated with the membranes in 5% milk/TBST. The proteins were quantified with Image Laboratory software version 3.0.

Statistical Analyses

Statistical analyses were performed using Stata statistical software (release 12.0; Stata Corporation, College Station, TX). Differences between co-twins were calculated by paired Wilcoxon signed rank tests. Correlations between mitochondrial and metabolic variables in all concordant and discordant twin individuals were calculated by using Pearson correlations, corrected for the clustered sampling of co-twins by survey methods (19) and adjusted for multiple comparisons by the number of principal components. The variables in Table 5 produced one principal component, which explained 88% of the variance. Therefore, the adjusted significance level for analyses in Table 5 was $P < 0.05$ divided by 1, that is, $P < 0.05$. Logarithmic corrections were used for non-normally distributed variables.

RESULTS

Characteristics of the twins are presented in Table 1. The obese (BMI 31.2 ± 1.0 kg/m^2) and the lean (25.3 ± 0.9 kg/m^2) co-twins of the discordant pairs (n = 26) had a mean difference of 18 ± 0.5 kg ($P < 0.001$) in body weight. The obese co-twins had significantly more SAT, VAT, and liver fat; larger adipocytes; higher plasma leptin levels; and lower plasma adiponectin levels; and were more insulin resistant than the lean co-twins. The concordant co-twins (n = 14) had similar body composition and metabolic measures (Table 1). As no differences in mitochondrial measures were found within the concordant pairs, results are presented only for the discordant pairs.

Downregulation of Mitochondrial-Related Transcripts in the SAT of Obese Co-twins

We first investigated the within-pair differences in the expression of mitochondrial proteins in SAT (n = 26) by linking the results from the transcriptomics data with those of MitoCarta. Among the 2,108 significantly differentially expressed genes, 222 genes were listed in MitoCarta (Supplementary Table 1). Most of these transcripts (187 of 222 transcripts, 84%) were downregulated in SAT of the obese co-twins compared with the lean co-twins. The top significantly upregulated and downregulated genes are shown in Table 2.

Downregulation of Key Mitochondrial Pathways in the SAT of Obese Co-twins

To investigate which functional entities the 222 mitochondrial transcripts represented, we subjected the transcripts to IPA. Among the most significantly different and downregulated pathways in the obese co-twins compared with the lean co-twins were the following key mitochondrial functions: OXPHOS ($P < 0.0001$), BCAA degradation

Table 1—Characteristics of the MZ twins

	Weight-discordant MZ pairs (ΔBMI >3 kg/m^2, n = 26 [n = 9 males, n = 17 females])		Weight-concordant MZ pairs (ΔBMI <3 kg/m^2, n = 14 [n = 9 males, n = 5 females])	
Variable	Lean co-twin	Obese co-twin	P value*	Both co-twins
Age (years)	29.9 ± 0.9	29.9 ± 0.9	0.33	31.6 ± 0.6
Weight (kg)	75.4 ± 3.5	93.3 ± 4.0	<0.0001	79.3 ± 2.5
Height (cm)	171.9 ± 2.0	172.2 ± 1.9	0.38	171.5 ± 2.0
BMI (kg/m^2)	25.3 ± 0.9	31.3 ± 1.0	<0.0001	26.9 ± 0.7
Body fat (%)	32.3 ± 1.8	41.1 ± 1.3	<0.0001	29.2 ± 1.7
Fat (kg)	24.9 ± 2.2	38.2 ± 2.1	<0.0001	23.5 ± 1.7
Fat-free mass (kg)	48.0 ± 2.1	52.1 ± 2.5	0.0001	53.4 ± 2.0
SAT (dm^3)	3,813.7 ± 416.8	6,358.9 ± 540.4	<0.0001	3,256.3 ± 261.2
VAT (dm^3)	790.2 ± 178.9	1,643.7 ± 247.4	<0.0001	1,065.2 ± 130.0
Liver fat (%)	1.12 ± 0.32	4.52 ± 0.99	<0.0001	2.87 ± 0.98
Adipocyte volume (pL)	355.6 ± 34	547 ± 59	0.0008	412.0 ± 46.2
Adipocyte number (10^{13})	8.4 ± 0.74	8.3 ± 0.60	0.95	7.82 ± 0.60
fP glucose (mmol/L)†	5.1 ± 0.1	5.3 ± 0.1	0.17	5.4 ± 0.1
fS insulin (mU/L)†	4.9 ± 0.5	8.5 ± 1.2	0.0011	5.5 ± 0.6
HOMA index†	1.1 ± 0.1	2.1 ± 0.3	0.0010	1.3 ± 0.2
Matsuda index†	8.6 ± 0.9	6.0 ± 0.7	0.0089	9.9 ± 1.3
AUC insulin in OGTT (mU/L)	87.6 ± 8.0	129.3 ± 24.6	0.031	77.5 ± 10.9
Total cholesterol (mmol/L)	4.4 ± 0.2	4.7 ± 0.2	0.14	4.5 ± 0.2
LDL cholesterol (mmol/L)	2.6 ± 0.1	3.0 ± 0.2	0.034	2.8 ± 0.2
HDL cholesterol (mmol/L)	1.6 ± 0.1	1.3 ± 0.1	0.0004	1.3 ± 0.1
Triglycerides (mmol/L)	0.94 ± 0.1	1.32 ± 0.2	0.014	1.02 ± 0.13
fP leptin (mg/mL)	18.9 ± 4.1	34.6 ± 5.5	0.0015	28.4 ± 10.2
fP adiponectin (μg/mL)	2.8 ± 0.3	2.2 ± 0.2	0.0023	2.2 ± 0.1
fS hs-CRP (mg/dL)	2.6 ± 0.7	4.0 ± 1.1	0.065	1.2 ± 0.3
Adipsin (ng/mL)	1,190 ± 45	1,310 ± 47	0.0063	1,070 ± 71
Total physical activity	8.9 ± 0.2	8.3 ± 0.2	0.213	8.9 ± 0.3
Sport index	3.2 ± 0.2	2.7 ± 0.2	0.061	3.3 ± 0.2
Leisure index	2.8 ± 0.1	2.8 ± 0.1	0.837	2.8 ± 0.1
Work index	2.8 ± 0.1	2.8 ± 0.1	0.466	2.8 ± 0.1

Data represent the mean ± SE. AUC, area under the curve; fP, fasting plasma; fS, fasting serum; OGTT, oral glucose tolerance test. *Wilcoxon rank sum test was used to compare values of the leaner vs. the heavier co-twin. †n = 25 obesity-discordant MZ pairs.

($P < 0.0001$), ketogenesis/ketolysis ($P < 0.0001$), the tricarboxylic acid cycle (TCA; $P < 0.0001$), glutaryl-CoA degradation ($P < 0.0001$), and fatty acid β-oxidation (FAO; $P < 0.0001$) (Table 3 and Supplementary Table 2).

Next we analyzed whether the most significant pathways were associated with obesity-related pathology by correlating the mean centroids of the pathways to measures of adiposity (SAT, VAT, and liver fat, adipocyte volume), insulin sensitivity (Matsuda index), insulin resistance (HOMA index), inflammation (adipsin, hs-CRP), leptin, and adiponectin. After multiple testing episodes, the mean centroid values of OXPHOS and TCA pathways correlated with SAT, VAT, liver fat, adipocyte volume, Matsuda and HOMA indexes, adipsin, and hs-CRP (Table 4). The TCA also correlated with adiponectin. Glutaryl-CoA degradation, ketogenesis, and tryptophan degradation pathways correlated with all of the selected clinical variables except adiponectin. BCAA degradation (valine, isoleucine, and leucine degradation pathways), FAO, and ketolysis correlated with all clinical variables.

Upstream Regulator Analysis

We performed IPA upstream regulator analysis to identify the transcriptional regulators that can explain the observed gene expression changes and pathways between the co-twins (n = 26) (20). We identified *FOXO1* ($P < 0.0001$), PGC-1α (*PPARGC1A*, $P < 0.0001$), PGC-1β (*PPARGC1B*, $P < 0.0001$), and lysine methyltransferase 2D (*KMT2D*, $P = 0.027$) (Table 5 and Supplementary Table 3) as the most significant upstream transcription factors

Table 2—Top upregulated and downregulated genes in the obese compared with the lean co-twins (n = 26 discordant pairs)

Symbol	Description	Adjusted P value	FC
Upregulated genes			
VAMP8	Vesicle-associated membrane protein 8	0.0041	1.51
HSPB7	Heat shock 27-kDa protein family, member 7 (cardiovascular)	0.0108	1.47
FTH1	Ferritin, heavy polypeptide 1	0.0003	1.41
TOMM40L	Translocase of outer mitochondrial membrane 40 homolog (yeast)-like	0.0012	1.38
TMEM160	Transmembrane protein 160	0.0037	1.33
PLA2G15	Phospholipase A2, group XV	0.0132	1.32
TXNRD1	Thioredoxin reductase 1	0.0016	1.30
SLC25A43	Solute carrier family 25, member 43	0.0018	1.24
Downregulated genes			
NIPSNAP3B	Nipsnap homolog 3B (*Caenorhabditis elegans*)	0.0002	−1.92
LDHD	Lactate dehydrogenase D	0.0025	−1.71
ALDH1L1	Aldehyde dehydrogenase 1 family, member L1	0.0010	−1.62
AASS	Aminoadipate-semialdehyde synthase	0.0006	−1.59
GPT2	Glutamic pyruvate transaminase (alanine aminotransferase) 2	0.0010	−1.58
ECHDC3	Enoyl-CoA hydratase domain containing 3	0.0006	−1.56
ALDH6A1	Aldehyde dehydrogenase 6 family, member A1	0.0006	−1.56
C10orf10	Chromosome 10 open reading frame 10	0.0186	−1.54
PXMP2	Peroxisomal membrane protein 2, 22 kDa	0.0004	−1.52
ACP6	Acid phosphatase 6, lysophosphatidic	0.0022	−1.48
PC	Pyruvate carboxylase	0.0015	−1.41
ECI1	Enoyl-CoA delta isomerase 1	0.0002	−1.41
PCCB	Propionyl CoA carboxylase, β-polypeptide	0.0006	−1.38
SHMT1	Serine hydroxymethyltransferase 1 (soluble)	0.0016	−1.38
ACACA	Acetyl-CoA carboxylase-α	0.0042	−1.37
LIAS	Lipoic acid synthetase	0.0010	−1.36
PCK2	Phosphoenolpyruvate carboxykinase 2 (mitochondrial)	0.0141	−1.35
HADH	Hydroxyacyl-CoA dehydrogenase	0.0002	−1.34

FC, fold change.

regulating the 222 transcripts. Based on the predicted z scores calculated in IPA, the biological activation state of all of these genes was lower in the obese co-twins compared with the lean co-twins. In our transcriptomics data, the expression level of PGC-1α was highly downregulated in the obese co-twins (lean 51.6 ± 5.1 arbitrary units [AU] vs. obese 34.1 ± 4.9 AU; arbitrary Affymetrix units, adjusted $P < 0.001$). The reduction of PGC-1α expression was verified with qRT-PCR (P = 0.004; Fig. 1). The expression of other upstream regulators was not different between the co-twins, but the expression levels of their target genes were reduced, suggesting post-transcriptional regulation (Table 5).

Differential Methylation of the Mitochondria-Related Transcripts and Upstream Regulators in the SAT of Obese Co-twins

Next, we investigated whether any of the 222 differentially expressed genes were also differentially methylated within the twin pairs, thus providing a potential molecular mechanism underlying the expression differences. Altogether, 130 CpG sites within 74 genes showed differential methylation ($P < 0.05$) within the discordant pairs (n = 24; Supplementary Table 5). Most of these sites (96 of 130 sites, 74%) were hypermethylated in the obese co-twins compared with the lean co-twins. When investigating the CpG sites in relation to CpG density, 89% (116 of 130 sites) were outside any CpG islands. Approximately half (68 of 130 sites, 52%) of the differentially methylated CpG sites were located in the gene bodies, and 42% (55 of 130 sites) were located in promoters. There was no difference between the promoter- and gene body–associated CpG sites in regard to their methylation status (hypermethylation vs. hypomethylation). We then explored whether there are any significant associations between the differentially expressed and methylated genes. Of the 74 genes, 40 showed significant correlation between expression and methylation (r = −0.24 to −0.70 and 0.25 to 0.44, $P < 0.05$) (Supplementary Table 6). There was in general an inverse relationship between expression and DNA methylation, and only 12 genes showed positive correlations.

Furthermore, we explored whether the methylation levels differed between the co-twins for the *PGC-1α* gene, the only upstream regulator that was differentially expressed between the co-twins. We found hypermethylation in the obese co-twins in two CpG sites within the gene body of *PGC-1α*, but no differences in other regions of the gene (Supplementary Table 5). Methylation in one of the CpG sites correlated significantly with PGC-1α expression (r = −0.31, P = 0.01) (Supplementary Table 6).

Reduction of mtDNA Amount, mtDNA-Encoded Transcripts, and MRP Transcripts in the SAT of Obese Co-twins

To further investigate the effect of obesity on mitochondrial amount and biogenesis in SAT, we measured the amount

Table 3—Pathways significantly changed in the obese compared with the lean co-twin (IPA of the differentially expressed genes, *n* = 26 discordant pairs)

Ingenuity canonical pathways	*P* value	Regulation	Molecules
OXPHOS	<0.0001	Downregulated	SDHB, COX6C, COX5B, NDUFB5, COX8A, ATP5L, ATP5G2, NDUFB8, ATP5S, NDUFA2, NDUFB10, NDUFS1, NDUFAB1, ATPAF1, ATP5I, COX4I1, NDUFA8, NDUFS4, ATP5O, ATP5A1, COX7C, NDUFS3, UQCRB, ATP5C1, COX11, NDUFB11, ATP5B, NDUFA6, CYC1, UQCRC2, COX7A2, NDUFA12, SDHD, UQCRC1
Valine degradation I	<0.0001	Downregulated	HADHB, HIBADH, BCKDHA, AUH, ACAD8, ACADSB, DBT, ALDH6A1, HADHA, BCKDHB
Glutaryl-CoA degradation	<0.0001	Downregulated	HADHB, ACAT2, ACAT1, HADHA, HADH, GCDH, HSD17B8
Isoleucine degradation I	<0.0001	Downregulated	HADHB, ACAT2, AUH, ACAD8, ACAT1, ACADSB, HADHA
Ketogenesis	<0.0001	Downregulated	HADHB, BDH1, ACAT2, ACAT1, HMGCL, HADHA
FAO I	<0.0001	Downregulated	HADHB, ECI2, AUH, ACADM, ECI1, HADHA, HADH, HSD17B8
Tryptophan degradation III (eukaryotic)	<0.0001	Downregulated	HADHB, ACAT2, ACAT1, HADHA, HADH, GCDH, HSD17B8
Ketolysis	<0.0001	Downregulated	HADHB, BDH1, ACAT2, ACAT1, HADHA
TCA II (eukaryotic)	<0.0001	Downregulated	SDHB, DHTKD1, SUCLG1, DLST, SDHD, FH, IDH3B
Leucine degradation I	<0.0001	Downregulated	AUH, MCCC1, HMGCL, ACADM, MCCC2

of mtDNA and the expression of mtDNA-encoded genes (12*S* rRNA, 16*S* rRNA, cytochrome c oxidase subunit 1 [COX1], NADH dehydrogenase subunit 5 [ND5], and CYTB, *n* = 15 discordant pairs). The mtDNA amount was reduced by ~20% (*P* = 0.031; Fig. 2*A*) in SAT of the obese co-twins compared with the lean co-twins. Significant negative correlations were observed between the mtDNA amount and HOMA (insulin resistance) and adipsin (inflammation) (Table 4).

Furthermore, mitochondrial 12*S* (*MT-RNR1*, *P* = 0.0064) and 16*S* (*MT-RNR2*, *P* = 0.0090) rRNAs, as well as mRNAs COX1 (*P* = 0.0064, CIV subunit), ND5 (*P* = 0.027, CI subunit), and CYTB (*P* = 0.0015, CIII subunit; Fig. 2*B*), were decreased in SAT of the obese co-twins compared with their lean counterparts. We also studied the expression of 30 nuclear transcripts for the MRPS and 50 nuclear transcripts for the MRPL of the mitochondrial ribosome using the Affymetrix data (*n* = 26 discordant pairs). In line with 12*S* and 16*S* rRNA expression, the average value of the total expression (a mean centroid) of both MRPS (lean 0.03 ± 0.09 AU vs. obese −0.31 ± 0.1 AU, $P < 0.001$) and MRPL (lean −0.04 ± 0.1 AU vs. obese −0.26 ± 0.1 AU, *P* = 0.0034) was lower in the obese compared with the lean co-twins (Fig. 2*C*).

Reduction of Mitochondrial Mass and OXPHOS Proteins in the SAT of Obese Twins

Finally, we measured mitochondrial content and the level of OXPHOS protein subunits in SAT lysates of seven discordant pairs by Western blot. Mitochondrial mass per cell (porin, a mitochondrial outer membrane protein compared with a cytoskeletal protein β-tubulin) trended downward in the obese co-twins (*P* = 0.09; Fig. 2*D* and *E*). Mitochondrial OXPHOS protein subunits of CIII, CIV, and CV were reduced in obesity: the level of CIII-core 2 (CIII subunit, *P* = 0.018), MT-CO1 (CIV subunit, *P* = 0.018), and CV-α (CV subunit, *P* = 0.028), compared with the levels of β-tubulin, were all lower in the obese co-twins than in the lean co-twins (Fig. 2*E*). As the different complex subunits typically follow the amounts of full holocomplexes, these results support deficiency of CIII, CIV, and CV. Fully nuclear-encoded CII did not differ between the co-twins. Furthermore, we analyzed whether the OXPHOS levels were reduced per mitochondria in obesity. Thus, we normalized the OXPHOS protein signals against the mitochondrial protein porin. The amount of CI (*P* = 0.063) trended downward, and complexes CIII (*P* = 0.018) and CIV (*P* = 0.028) were reduced in the obese co-twins (Fig. 2*E*). Overall, the protein results suggest a trend of lower mitochondrial mass (porin) and a decrease of OXPHOS levels per cell and per mitochondria as a downstream effect of the reduced mtDNA amount (Fig. 3).

Hyperplastic Versus Hypertrophic Obesity

Because the mitochondrial pathways had significant negative correlations with adipocyte volume ($P < 0.01$, Table 4), we analyzed whether the mitochondrial measures differed in discordant pairs with hyperplastic versus hypertrophic pattern of adipocyte morphology. In the discordant pairs where the obese co-twins had a solely hypertrophic pattern (larger and fewer adipocytes than their co-twins), the obese co-twins had a significantly reduced amount of mtDNA compared with their lean co-twins (lean 1.05 ± 0.7 vs. obese 0.82 ± 0.07, *P* = 0.028), but no other differences in the mitochondrial measures were found between the two groups.

Sex, Onset of Obesity Discordance, Family History, and Lifestyle Factors in the Discordant Pairs

The within-pair differences in all measures of adiposity and metabolism (Table 1), as well as those in mitochondrial measures, were similar in males and females. The mean

age at the onset of obesity discordance was 22.6 ± 0.6 years. Consequently, the length of obesity discordance was on average 6.3 ± 0.3 years. Of the total 44 parents of the discordant pairs for whom data were available, 15.9% were obese (4 of 23 of the mothers and 3 of 21 of the fathers), including one twin pair where both parents were obese. The parents were examined when the twins were 16 years of age. The age of the mothers was 42.2 ± 0.7 years, and that of the fathers, 45.4 ± 0.8 years. The total as well as sport, leisure time, and work physical activity levels of the obese and the lean co-twins were similar (Table 1), and did not correlate with mitochondrial measures.

DISCUSSION

We performed a comprehensive set of experiments to test a hypothesis that mitochondrial biogenesis is downregulated in human SAT in obesity. We used a unique study design: rare MZ weight-discordant twin pairs, which enabled us to control for sex, age, and genetic background between the lean and the obese groups—a major advantage for conclusions regarding a multifactorial trait such as obesity. We demonstrate a widespread reduction in the expression of both mitochondrial- and nuclear-encoded mitochondrial genes leading to downregulation of mitochondrial biogenesis in SAT of the obese twins compared with their leaner co-twins. Many of the differentially expressed transcripts were also differentially methylated within the twin pairs. Reduction of the mitochondrial oxidative metabolism in SAT correlated with whole-body insulin resistance and inflammation. Our findings provide evidence of a substantial insufficiency of mitochondrial biogenesis in SAT in acquired obesity that already exists prior to the onset of clinical metabolic complications.

The OXPHOS system is unique because it is encoded by both the nuclear and the mitochondrial genome. We showed that mtDNA, its transcripts, OXPHOS subunits, as well as nuclear genes encoding OXPHOS proteins are reduced in the obese co-twins, suggesting a major downregulation in mitochondrial oxidative ATP production and catabolic functions in SAT in acquired obesity. A similar reduction of mtDNA in SAT in obesity has been found in previous studies by us (10) and others (21), but the generalized downregulation of mitochondrial proteins and metabolism has not been reported previously. After mtDNA transcription, mitochondria translate their mRNAs on mitochondrial ribosomes that comprise two mtDNA-encoded rRNAs and >80 nuclear-encoded proteins (22). We report an extensive reduction in the transcript levels of rRNAs and MRPs, emphasizing the downregulation of the translation machinery of both the nuclear and mitochondrial expression systems. These findings are in agreement with previous findings in two mouse models of obesity and type 2 diabetes, which showed a low abundance of MRP transcripts and mitochondrial biogenesis in inguinal adipose tissue (23), as well as in a rat model for late-onset obesity, in which a truncation of MRPS26 was associated with the accumulation of visceral fat and insulin sensitivity (24).

Table 4—Correlations of mitochondrial variables with metabolic measures in individual MZ twins (n = 80)

	SAT	VAT	Liver fat	Adipocyte volume	Matsuda index	HOMA	fP-leptin	fP-adiponectin	hs-CRP	Adipsin
mtDNA	−0.2544	−0.0835	−0.1761	−0.2076	0.2954	−0.4582*	−0.2413	−0.0408	−0.0166	−0.4007*
OXPHOS	−0.367†	−0.603‡	−0.420†	−0.497†	0.445‡	−0.322†	−0.191	0.353*	−0.384†	−0.3402*
FAO	−0.622‡	−0.669‡	−0.518‡	−0.584‡	0.669‡	−0.595‡	−0.519‡	0.378†	−0.476‡	−0.4174†
TCA	−0.315†	−0.660‡	−0.432†	−0.452†	0.483‡	−0.388‡	−0.147	0.456‡	−0.416‡	−0.4241†
Glutaryl-CoA degradation	−0.690‡	−0.644‡	−0.469‡	−0.586‡	0.634‡	−0.558‡	−0.543‡	0.330*	−0.470‡	−0.4484‡
Ketogenesis	−0.661‡	−0.652‡	−0.480‡	−0.569‡	0.623‡	−0.570‡	−0.488†	0.358*	−0.437†	−0.4337‡
Ketolysis	−0.657‡	−0.627‡	−0.478‡	−0.541†	0.626‡	−0.587‡	−0.490†	0.387*	−0.437†	−0.4671‡
Valine degradation	−0.585‡	−0.702‡	−0.559‡	−0.596‡	0.658‡	−0.638‡	−0.425†	0.524‡	−0.486‡	−0.5377‡
Leucine degradation	−0.430†	−0.649‡	−0.485‡	−0.489†	0.578‡	−0.506‡	−0.306†	0.411†	−0.412‡	−0.4003†
Isoleucine degradation	−0.533‡	−0.641‡	−0.472‡	−0.512‡	0.602‡	−0.581‡	−0.391*	0.486‡	−0.430‡	−0.5187‡
Tryptophan degradation	−0.630‡	−0.644‡	−0.469‡	−0.586‡	0.634‡	−0.558‡	−0.543‡	0.330*	−0.470‡	−0.4484‡

fP, fasting plasma. *$P < 0.05$, †$P < 0.01$, ‡$P < 0.001$.

Table 5—Upstream transcription factors regulating the mitochondrial-related genes (IPA of the differentially expressed genes, *n* = 26 discordant pairs)

Upstream regulator	Predicted activation state	Activation *z* score	*P* value of overlap	Target molecules in the dataset
FOXO1	Inhibited	−3.162	4.42e-06	↓ ACACA, ↓ ATP5B, ↓ MAVS, ↓ MRPL45, ↓ MRPL46, ↓ MRPL57, ↓ MRPS18A, ↓ MRPS2, ↓ MRPS22, ↓ MRPS30, ↓ MRPS7, ↓ NDUFA12, ↓ NDUFA8, ↓ PDHB
PPARGC1A	Inhibited	−2.823	3.28e-09	↓ ACACA, ↓ ACACB, ↓ ACADM, ↑ ALAS1, ↓ ATP5B, ↓ ATP5O, ↓ COX4I1, ↓ NDUFB5, ↓ NDUFS1, ↓ PDK4, ↓ TXN2
KMT2D	Inhibited	−2.236	0.0272	↓ ACADM, ↓ ECI2, ↓ HDDC2, ↓ OXR1, ↓ SFXN4
PPARGC1B	Inhibited	−2.219	7.19e-06	↓ ACACA, ↓ ACACB, ↓ ACADM, ↓ COX4I1, ↓ PDK4
KLF15	Inhibited	−2.121	1.29e-09	↓ ACADM, ↓ DECR1, ↓ HADHA, ↓ HADHB, ↓ MLYCD, ↓ PDK4, ↓ PXMP2, ↑ SLC25A20
HNF1A	Inhibited	−2.000	0.0062	↓ CCBL2, ↓ COQ7, ↓ FH, ↑ GARS, ↓ MCCC1, ↓ PDK1, ↓ SFXN2, ↓ UQCRC2

↓, downregulated in the obese compared with the lean co-twins; ↑, upregulated in the obese compared with the lean co-twins.

Finally, the OXPHOS complexes, partially encoded by mtDNA, were downregulated without a significant decrease of mitochondrial mass (porin/tubulin), showing that the mitochondrial OXPHOS levels within the cell and within the mitochondria are reduced in the SAT of the obese co-twins.

Pathway analysis of nuclear-encoded mitochondrial transcripts revealed changes in mitochondrial oxidative pathways, including FAO, TCA, ketogenesis, ketolysis, and BCAA degradation pathways in the obese co-twins. We found that a downregulation in oxidative metabolic pathways in SAT inversely correlated with several clinical parameters. Mitochondrial pathways correlated negatively with all adiposity measures, insulin resistance, and inflammation and correlated positively with adiponectin levels. We also observed that the larger the adipocyte volume, the more severe was the decrease in mitochondrial oxidative metabolic pathways. Recently, it has been proposed that a decrease in mitochondrial oxidative metabolism measured by oxygen consumption rate in isolated adipocytes is caused by obesity rather than the adipocyte size (8). Our study design controls for genetic factors between the obese and the lean groups and suggests that the hypertrophic but not the hyperplastic pattern of obesity relates to decreased mtDNA amount. Thus, our findings are in line with previous studies (16,25–27) reporting associations between hypertrophy and metabolic abnormalities.

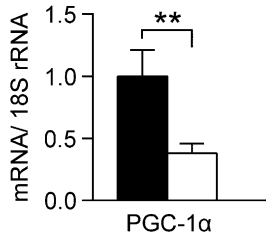

Figure 1—Reduction of PGC-1α in SAT of the obese MZ twins. Reduced expression of PGC-1α was confirmed by qRT-PCR in the SAT of the MZ obese compared with the lean co-twins (*n* = 15 discordant pairs). The bars indicate the mean with SE. ***P* < 0.01 (*t* test).

Although mitochondrial function and the development of type 2 diabetes are suggested to be linked (28), previous studies on mitochondrial biogenesis in relation to insulin sensitivity in adipocytes and adipose tissue in human subjects are surprisingly few. In one study (29), the exposure of 3T3-L1 mouse preadipocytes to high levels of glucose and free fatty acids resulted in decreased mitochondrial size and membrane potential and in the downregulation of PGC-1α, indicating mitochondrial dysfunction. In another study (30), high-fat feeding of rats resulted in impaired glucose homeostasis and decreased PGC-1α expression, mtDNA content, and CI and CIV protein levels in epididymal adipose tissue. These studies supported a relationship between abundant glucose or fatty acids, decreased mitochondrial function, and impaired glucose tolerance, whereas studies on mouse adipocytes did not confirm a causal link between reduced mitochondrial biogenesis and impaired whole-body glucose homeostasis (31). Our study, combining molecular analysis of mtDNA metabolism with mitochondrial pathway analyses, suggests that impaired mitochondrial biogenesis in SAT in humans is related to insulin resistance and to other mild metabolic alterations already present before the clinical diagnosis of type 2 diabetes or other obesity-related diseases.

PGC-1α was the only predicted upstream regulator whose expression was different between the co-twins. PGC-1α is a transcription coactivator and a master regulator of mitochondrial biogenesis that controls and coordinates the expression of nuclear and mitochondrial genes in white adipocytes (32–35). Low PGC-1α expression in SAT has also been found to correlate with increased BMI (21) and to be associated with morbid obesity (6), type 2

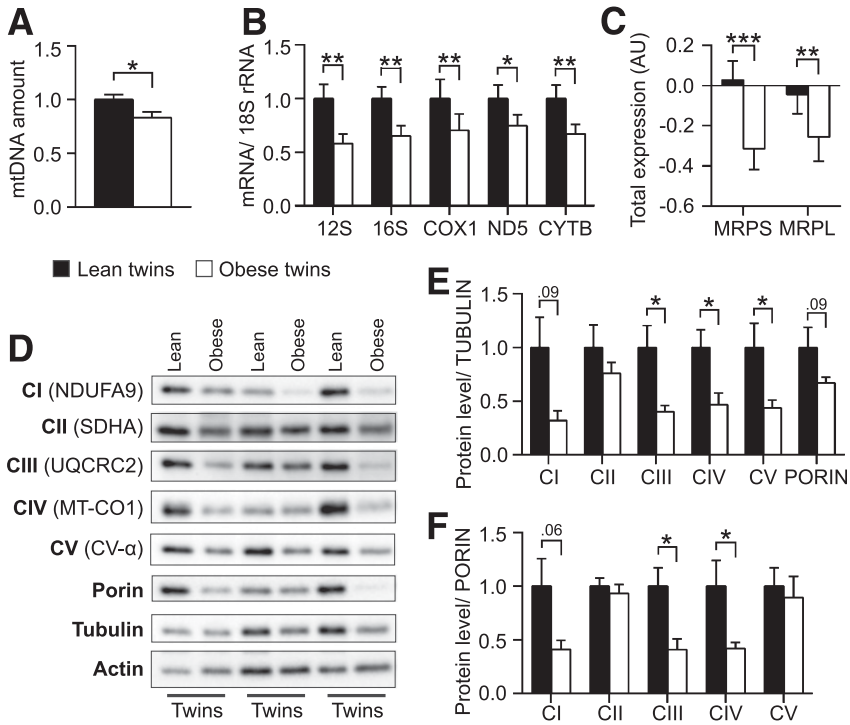

Figure 2—Reduction of mtDNA amount, mtDNA transcripts, MRPS/MRPL, and OXPHOS protein amounts in SAT of obese MZ twins. Relative mtDNA amount measured by qPCR (*A*) and mtDNA transcripts measured by qRT-PCR (*B*) in SAT of the MZ obese compared with the lean co-twins (n = 15 discordant pairs). *C*: The mean centroid values of MRPS and MRPL in the SAT of the obese compared with the lean co-twins (n = 26 discordant pairs). *D*: Western blot analysis of SAT lysates. *E* and *F*: Relative amount of OXPHOS proteins in the SAT (n = 7 discordant pairs). Western blot signals were normalized against β-tubulin (*E*) and porin (*F*). The bars indicate the mean with SE. $^*P < 0.05$, $^{**}P < 0.01$, $^{***}P < 0.001$ (paired Wilcoxon signed rank test).

diabetes (5), and insulin resistance (7). PGC-1α–responsive OXPHOS genes showed reduced expression in VAT in type 2 diabetes (36). Fat-specific PGC-1α knockout mice displayed a significant reduction in transcripts of OXPHOS, FAO, and TCA genes in inguinal SAT, and developed glucose intolerance and insulin resistance when challenged with a high-fat diet, demonstrating the necessity of oxidative metabolism in fat for whole-body metabolism (37). FOXO1 was the first predicted upstream regulator of our 222 transcripts. The expression of FOXO1 has been shown (38) to be downregulated in VAT compared with SAT of obese and nonobese individuals, and its protein levels reduced in a dose-dependent manner in 3T3-L1 adipocytes treated with free fatty acids

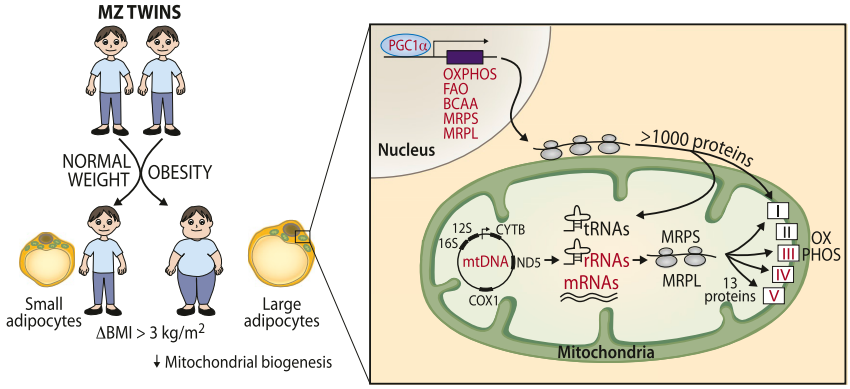

Figure 3—Downregulation of mitochondrial biogenesis in the SAT of MZ obese co-twins. Twenty-six weight-discordant healthy young MZ twin pairs (ΔBMI >3 kg/m^2) were enrolled in the study. Red denotes the downregulated transcript protein subunits in the obese co-twins compared with their lean co-twins. In addition, 222 of >1,000 nuclear-encoded mitochondrial genes were downregulated. 12S, 12S rRNA; 16S, 16S rRNA; I–V, OXPHOS protein complexes I–V.

as well as in intraperitoneal adipose tissue of *db/db* mice (39). We did not find significantly changed FOXO1 transcript levels, but FOXO1 and also PGC-1α are post-translationally regulated (40,41), and therefore the transcript levels do not fully reflect the gene activity. We show that three CpG sites in the body of PGC-1α were hypermethylated in the obese co-twins. This hypermethylation correlated negatively with gene expression, suggesting that DNA methylation may reduce the transcription of the gene. Previous studies (42) have reported that compared with the lean controls, obese patients with type 2 diabetes have a PGC-1α promotor hypermethylation in SAT. Our data also show that 74 of the 222 differentially expressed genes targeting mitochondria are differentially methylated between the co-twins, and in general inversely correlated with expression. This poses an interesting possibility that epigenetic modifications in certain nuclear genes associate with the decrease in mitochondrial biogenesis in SAT in acquired obesity. In obesity-discordant MZ twins, such an effect is acquired, and independent of the genetic background.

Healthy young adult MZ twins discordant for obesity are extremely rare, as they share both genes and family. We succeeded in finding 26 highly discordant pairs—mainly in their third decade of life, with relatively recent onset of weight discordance—from 10 birth cohorts of Finnish twins. Because the twins are matched on multiple factors, including genes, our study has increased power over a study comparing unrelated obese and lean subjects. Our study is cross-sectional and therefore does not allow definitive conclusions about causality. However, genetic variants and shared exposures/experiences can be excluded as confounders of the observed associations. All analyses in this study were performed with whole SAT biopsy samples that include stroma-vascular fraction cells, the contribution of which cannot be distinguished from that of the adipocytes.

In summary, we observed strong evidence for an association between acquired obesity and downregulation of mitochondrial biogenesis in SAT. Our findings suggest that obesity is related to suppressed mitochondrial oxidative activity in SAT. Importantly, we showed that the downregulation of mitochondrial biogenesis and oxidative metabolic pathways in SAT is a phenomenon in obesity associated with a range of mild metabolic alterations, insulin resistance, and low-grade inflammation. The genes targeting mitochondria may be epigenetically regulated. These data suggest that obesity-related disease development may be halted by improving mitochondrial activity in SAT.

Acknowledgments. The authors thank the twins for their invaluable contributions to the study. The authors also thank Barbara Every, of BioMedical Editor, for English language editing, and Eija Pirinen for her valuable comments.

Funding. The study was supported by Helsinki University Hospital Research Funds and by grants from the Novo Nordisk Foundation, the Diabetes Research Foundation, the Jalmari and Rauha Ahokas Foundation, the Finnish Foundation for Cardiovascular Research (for K.H.P.), the Academy of Finland (A.S.; grants 265240 and 263278 for J.K.; grants 272376 and 266286 for K.H.P.), the Orion Foundation (for S.H.), the University of Helsinki, the European Research Council, and the Sigrid Jusélius Foundation (for A.S.).

Duality of Interest. No potential conflicts of interest relevant to this article were reported.

Author Contributions. S.H. performed and designed the research, collected and analyzed the data, and wrote the manuscript. J.B. performed and designed the research, analyzed the data, and wrote the manuscript. M.M. performed the transcriptomics data analysis. R.K., J.K., and A.R. participated in the revision of the work. M.O. wrote the epigenetic analyses. K.I. performed the epigenetic analyses. A.H., J.L., and N.L. participated in the imaging of the twins. K.V. and E.M. participated in analyzing adiponectin and leptin. A.S. designed the research, supervised the work, and participated in the revision and discussion of the results. K.H.P. designed the research, supervised the work, collected the data, and participated in the revision and discussion of the results. K.H.P. is the guarantor of this work and, as such, had full access to all the data in the study and takes responsibility for the integrity of the data and the accuracy of the data analysis.

References

1. De Pauw A, Tejerina S, Raes M, Keijer J, Arnould T. Mitochondrial (dys)function in adipocyte (de)differentiation and systemic metabolic alterations. Am J Pathol 2009;175:927–939

2. Falkenberg M, Larsson NG, Gustafsson CM. DNA replication and transcription in mammalian mitochondria. Annu Rev Biochem 2007;76:679–699

3. Nunnari J, Suomalainen A. Mitochondria: in sickness and in health. Cell 2012;148:1145–1159

4. Pagliarini DJ, Calvo SE, Chang B, et al. A mitochondrial protein compendium elucidates complex I disease biology. Cell 2008;134:112–123

5. Bogacka I, Xie H, Bray GA, Smith SR. Pioglitazone induces mitochondrial biogenesis in human subcutaneous adipose tissue in vivo. Diabetes 2005;54:1392–1399

6. Semple RK, Crowley VC, Sewter CP, et al. Expression of the thermogenic nuclear hormone receptor coactivator PGC-1alpha is reduced in the adipose tissue of morbidly obese subjects. Int J Obes Relat Metab Disord 2004;28:176–179

7. Hammarstedt A, Jansson PA, Wesslau C, Yang X, Smith U. Reduced expression of PGC-1 and insulin-signaling molecules in adipose tissue is associated with insulin resistance. Biochem Biophys Res Commun 2003;301:578–582

8. Yin X, Lanza IR, Swain JM, Sarr MG, Nair KS, Jensen MD. Adipocyte mitochondrial function is reduced in human obesity independent of fat cell size. J Clin Endocrinol Metab 2014;99:E209–E216

9. Yehuda-Shnaidman E, Buehrer B, Pi J, Kumar N, Collins S. Acute stimulation of white adipocyte respiration by PKA-induced lipolysis. Diabetes 2010;59:2474–2483

10. Pietiläinen KH, Naukkarinen J, Rissanen A, et al. Global transcript profiles of fat in monozygotic twins discordant for BMI: pathways behind acquired obesity. PLoS Med 2008;5:e51

11. Mustelin L, Silventoinen K, Pietiläinen K, Rissanen A, Kaprio J. Physical activity reduces the influence of genetic effects on BMI and waist circumference: a study in young adult twins. Int J Obes (Lond) 2009;33:29–36

12. Kaprio J. Twin studies in Finland 2006. Twin Res Hum Genet 2006;9:772–777

13. Granér M, Seppälä-Lindroos A, Rissanen A, et al. Epicardial fat, cardiac dimensions, and low-grade inflammation in young adult monozygotic twins discordant for obesity. Am J Cardiol 2012;109:1295–1302

14. Naukkarinen J, Heinonen S, Hakkarainen A, et al. Characterising metabolically healthy obesity in weight-discordant monozygotic twins. Diabetologia 2014;57:167–176

15. Pietrobelli A, Formica C, Wang Z, Heymsfield SB. Dual-energy X-ray absorptiometry body composition model: review of physical concepts. Am J Physiol 1996;271:E941–E951

16. Heinonen S, Saarinen L, Naukkarinen J, et al. Adipocyte morphology and implications for metabolic derangements in acquired obesity. Int J Obes (Lond) 2014;38:1423–1431

17. Gentleman RC, Carey VJ, Bates DM, et al. Bioconductor: open software development for computational biology and bioinformatics. Genome Biol 2004;5: R80
18. Ritchie ME, Phipson B, Wu D, et al. limma powers differential expression analyses for RNA-sequencing and microarray studies. Nucleic Acids Res 2015; 43:e47
19. Rao J, Scott A. On chi-squared tests for multiway contingency tables with cell proportions estimated from survey data. Ann Stat 1984;12:46–60
20. Krämer A, Green J, Pollard J Jr, Tugendreich S. Causal analysis approaches in ingenuity pathway analysis. Bioinformatics 2014;30:523–530
21. Kaaman M, Sparks LM, van Harmelen V, et al. Strong association between mitochondrial DNA copy number and lipogenesis in human white adipose tissue. Diabetologia 2007;50:2526–2533
22. Attardi G, Schatz G. Biogenesis of mitochondria. Annu Rev Cell Biol 1988;4: 289–333
23. Rong JX, Qiu Y, Hansen MK, et al. Adipose mitochondrial biogenesis is suppressed in db/db and high-fat diet-fed mice and improved by rosiglitazone. Diabetes 2007;56:1751–1760
24. Bains RK, Wells SE, Flavell DM, et al. Visceral obesity without insulin resistance in late-onset obesity rats. Endocrinology 2004;145:2666–2679
25. Weyer C, Foley JE, Bogardus C, Tataranni PA, Pratley RE. Enlarged subcutaneous abdominal adipocyte size, but not obesity itself, predicts type II diabetes independent of insulin resistance. Diabetologia 2000;43:1498–1506
26. Salans LB, Knittle JL, Hirsch J. The role of adipose cell size and adipose tissue insulin sensitivity in the carbohydrate intolerance of human obesity. J Clin Invest 1968;47:153–165
27. Lönn M, Mehlig K, Bengtsson C, Lissner L. Adipocyte size predicts incidence of type 2 diabetes in women. FASEB J 2010;24:326–331
28. Turner N, Heilbronn LK. Is mitochondrial dysfunction a cause of insulin resistance? Trends Endocrinol Metab 2008;19:324–330
29. Gao CL, Zhu C, Zhao YP, et al. Mitochondrial dysfunction is induced by high levels of glucose and free fatty acids in 3T3-L1 adipocytes. Mol Cell Endocrinol 2010;320:25–33
30. Sutherland LN, Capozzi LC, Turchinsky NJ, Bell RC, Wright DC. Time course of high-fat diet-induced reductions in adipose tissue mitochondrial proteins: potential mechanisms and the relationship to glucose intolerance. Am J Physiol Endocrinol Metab 2008;295:E1076–E1083
31. Enguix N, Pardo R, González A, et al. Mice lacking PGC-1β in adipose tissues reveal a dissociation between mitochondrial dysfunction and insulin resistance. Mol Metab 2013;2:215–226
32. Puigserver P, Spiegelman BM. Peroxisome proliferator-activated receptor-gamma coactivator 1 alpha (PGC-1 alpha): transcriptional coactivator and metabolic regulator. Endocr Rev 2003;24:78–90
33. Scarpulla RC. Nuclear activators and coactivators in mammalian mitochondrial biogenesis. Biochim Biophys Acta 2002;1576:1–14
34. Tiraby C, Tavernier G, Lefort C, et al. Acquirement of brown fat cell features by human white adipocytes. J Biol Chem 2003;278:33370–33376
35. Wilson-Fritch L, Nicoloro S, Chouinard M, et al. Mitochondrial remodeling in adipose tissue associated with obesity and treatment with rosiglitazone. J Clin Invest 2004;114:1281–1289
36. Dahlman I, Forsgren M, Sjögren A, et al. Downregulation of electron transport chain genes in visceral adipose tissue in type 2 diabetes independent of obesity and possibly involving tumor necrosis factor-alpha. Diabetes 2006;55: 1792–1799
37. Kleiner S, Mepani RJ, Laznik D, et al. Development of insulin resistance in mice lacking PGC-1α in adipose tissues. Proc Natl Acad Sci USA 2012;109: 9635–9640
38. Hammes TO, Costa Cdos S, Rohden F, et al. Parallel down-regulation of FOXO1, PPARγ and adiponectin mRNA expression in visceral adipose tissue of class III obese individuals. Obes Facts 2012;5:452–459
39. Subauste AR, Burant CF. Role of FoxO1 in FFA-induced oxidative stress in adipocytes. Am J Physiol Endocrinol Metab 2007;293:E159–E164
40. Li X, Monks B, Ge Q, Birnbaum MJ. Akt/PKB regulates hepatic metabolism by directly inhibiting PGC-1alpha transcription coactivator. Nature 2007;447:1012–1016
41. Barthel A, Schmoll D, Unterman TG. FoxO proteins in insulin action and metabolism. Trends Endocrinol Metab 2005;16:183–189
42. Chen M, Macpherson A, Owens J, Wittert G, Heilbronn LK. Obesity alone or with type 2 diabetes is associated with tissue specific alterations in DNA methylation and gene expression of PPARGC1A and IGF2. J Diabetes Res Clin Metab 2012;1:1–8